POLITECNICO DI TORINO
Repository ISTITUZIONALE

The role of soil amendments in limiting the leaching of agrochemicals: Laboratory assessment for copper sulphate and dicamba

Original
The role of soil amendments in limiting the leaching of agrochemicals: Laboratory assessment for copper sulphate and dicamba / Granetto, M., Bianco, C., Tosco, T.. - In: JOURNAL OF CLEANER PRODUCTION. - ISSN 0959-6526. - ELETTRONICO. - 474:(2024). [10.1016/j.jclepro.2024.143532]

Availability:
This version is available at: 11583/2994765 since: 2025-01-07T09:53:47Z

Publisher:
Elsevier Ltd

Published
DOI:10.1016/j.jclepro.2024.143532

Terms of use:

This article is made available under terms and conditions as specified in the corresponding bibliographic description in the repository

Publisher copyright
Elsevier postprint/Author's Accepted Manuscript

© 2024. This manuscript version is made available under the CC-BY-NC-ND 4.0 license http://creativecommons.org/licenses/by-nc-nd/4.0/.The final authenticated version is available online at: http://dx.doi.org/10.1016/j.jclepro.2024.143532

(Article begins on next page)

16 November 2026

The role of soil amendments in limiting the leaching of agrochemicals: laboratory assessment for copper sulphate and dicamba

Monica Granetto, Carlo Bianco, Tiziana Tosco*

Department of Environmental, Land and Infrastructure Engineering (DIATI), Politecnico di Torino, Corso Duca degli Abruzzi, 24, 10129, Turin, Italy

* *Corresponding author:* tiziana.tosco@polito.it

Submitted to Journal of Cleaner Production

Abstract

Agriculture is among the major contributors to soil and groundwater pollution, primarily through the widespread leaching of pesticides and fertilizers from crops, as well as accidental releases from point sources. Therefore, alongside restrictions on the use of highly soluble agrochemicals and enhanced application guidelines, there is a significant demand for low-impact and cost-effective solutions aimed at reducing the mobility of agrochemicals in the soils. This study evaluates the potential of soil amendments—commonly used to enhance soil structural properties, water holding capacity, and fertility—to also absorb highly soluble pesticides, thereby controlling their leaching into the subsoil. Specifically, zeolite, biochar, and milled corncob were examined in laboratory tests under static (batch tests) and dynamic (column leaching tests) conditions to assess their effectiveness in adsorbing two widely used pesticides, copper sulphate and dicamba. Batch adsorption tests were performed using the amendments as pure materials and in mixtures with sand at various application rates (1 to 20% by weight). The highest affinity to copper sulphate was recorded for biochar, while dicamba exhibited a higher affinity to corncob, thanks to its higher content of organic carbon. Column leaching tests, performed at an amendment application rate of 5%, confirmed the different affinity observed in batch tests among pesticides and amended soil. Less than 2% of copper sulphate leached out from biochar- and zeolite-sand columns, while a recovery of 10% and 56% was observed for the corncob-sand mixture and for pure sand, respectively. Dicamba leaching from biochar- and corncob-sand columns was halved compared to pure sand. In conclusion, the tested soil amendments resulted highly effective in reducing pesticide leaching, opening the way for their possible applications in agriculture to reduce or prevent both diffuse and punctual contamination.

Keywords

Soil amendments; Zeolite; Biochar; Corncob; Pesticide leaching; Pesticide sorption

Highlights

Biochar and corncob show high affinity to dicamba and limit its leaching in lab tests

Zeolite-amended sand highly retain Cu sulphate and retention is partly irreversible

Unprocessed agricultural waste can effectively control leaching of organic pesticides

Introduction

Preserving the high quality of surface water and groundwater represents a current global challenge. Agriculture, along with urban and industrial activities, is among the major pollution sources (Sethi and Di Molfetta, 2019), including both diffuse emissions associated with excessive load of nutrients (in particular phosphorus and nitrogen), pesticides and pharmaceuticals (Dordio and Carvalho, 2013), and accidental spills at well-localized contamination roots (e.g. storage vessels or sprayer tanks, parking or loading areas, etc.) (Ritter, 1988). Several technologies are currently available to manage point source releases and treat collected streams of contaminated water, similar to those applied to industrial or civil effluents. Conversely, controlling contaminant spread from diffuse sources is an intrinsically challenging target. To this aim, soil amendments, in particular processed or raw agricultural waste (e.g. sawdust, mowing, biochar, etc.) and minerals (e.g. zeolites) show good potential (Ahmad et al., 2014; Sud et al., 2008). Their effectiveness in adsorbing and/or immobilizing organic and inorganic contaminants is already exploited in industrial wastewater treatments and remediation of contaminated soils and sediments (Cao et al., 2011; Ghosh et al., 2011). Conversely, in the agricultural sector, their primary use is currently as soil quality improvers, to increase soil water retention capacity and control fertilizer release to plants (Diacono and Montemurro, 2010). Surprisingly, little attention has been devoted so far to their potential interactions with pesticides, and more in general to limit contaminant release from agricultural sources (Kookana et al., 2011). Among the limited literature available on this topic, notable findings include the biochar capacity to increase glyphosate adsorption (with a partition coefficient 33% higher in biochar-amended soil than in untreated soil) (Kumari et al., 2016) and the ability of Ca-hydroxide, Ca-bentonite, and natural zeolites to significantly increase the copper immobilization compared to control soil (Lahori et al., 2017). Moreover, the leaching potential of fipronil, a broad spectrum insecticide, was reduced by 97% in in coarse sand amended with cereal straw, compared to the unamended soil (Joshi et al., 2016). In this framework, this study intends to advance knowledge on the role of soil amendments in controlling leaching of soluble agrochemicals.

Among adsorbents derived from agricultural waste, biochar, produced through pyrolysis of plant residues, is the most known and used soil amendment. Its porous structure and surface properties render it an effective,

low cost material for removal of both organic (Tong et al., 2019) and inorganic compounds (Liu et al., 2022). Similar advantages could be obtained also with mineral amendments like zeolites, whose exploitation in agriculture increased in the last two decades (Mondal et al., 2021). Zeolites, sometimes after surface modification, are often used in industrial wastewater treatments in deep bed filtration, and as soil amendments for nutrients adsorption and controlled release (Ferretti et al., 2020; Wang and Wang, 2022). However, only a few studies investigated their adsorption capacity toward agricultural contaminants such as pesticides (Cataldo et al., 2021).

Despite the good performance of biochar and zeolites as adsorbents, their production processes (either biochar pyrolysis or zeolite mining), milling and surface functionalization require non negligible energy input. Consequently, in the name of a higher sustainability, perspective soil amendments produced from agricultural waste with minimal energy demand would be highly desired. Milled corncob, with its large availability and highly porous structure, is a promising option. It is currently exploited mainly for its high energy content and as a source for biochar production, but to the authors' knowledge no previous study is available on the efficacy of unprocessed corncob as an adsorbent. For this reason, it has been selected along with biochar and zeolite to be investigated in this study.

Copper sulphate and dicamba, both characterized by high solubility and thus leaching potential, were studied in this work as representative of, respectively, inorganic and organic pesticides. Copper, broadly used as fungicide in organic agriculture, is among the priority pollutants categorized by USEPA. Copper leaching is influenced by the precipitation intensity and duration, the chemistry of infiltrating water (ionic strength, pH), and the presence and dynamics of dissolved organic matter (DOM), which has a high affinity with copper (Aldrich et al., 2002). High infiltration was reported in sandy soils, with 47.9% of copper leaching from columns spiked with 600 mg kg^{-1} of Cu (Bakshi et al., 2014). Dicamba, an herbicide targeting broadleaf weeds in crops like maize and sorghum, is highly soluble in water, with consequent high leaching potential (Granetto et al., 2022). Its use in conjunction with 2,4-D has increased in USA since 2002 in response to the notable rise in the number of herbicide-resistant weed biotypes (Hoy et al., 2015). Moreover, the introduction of

dicamba-resistant crops, such as soybeans and cotton, in Brazil (CTNBio, 2023) and other parts of the world, suggests an overall increase in the application of this herbicide in the next years (Aguiar et al., 2023).

This research presents laboratory studies on the potentiality of soil amendments in limiting the leaching of soluble pesticides in static (batch tests) and dynamic conditions (column leaching tests), elucidating the dependence of adsorption mechanisms and removal efficiency on morphology, composition and physical-chemical properties and application ratio of the amendments. Despite the laboratory scale of the study, a few preliminary conclusions were drawn in view of a full-scale application of the studied amendments for pesticide immobilization.

Materials and methods

Materials

Three natural amendments were supplied by local producers, including biochar (Ronda Engineering; nominal size < 5mm; source: pyrolysis at 700 °C of untreated woodworking waste), zeolite (Zeocel Italia; nominal size: 0.6-2mm; nominal composition: 70±5% chabazite, 2±1 % phillipsite, 5±2% sanidine, 3±1% augite, 2±1% illite), and corncob (Agrindustria; nominal size: 50% 180-610µm and 50% 610-850µm; source: fibrous part of the corn ear after extraction, drying and milling).

Silica sand (Dorsilit 8, Dorfner, Germany; d_{10}, d_{50} and d_{90} equal respectively to 0.415, 0.45 and 0.5 mm) was used to mimic the soil structure, as pure material or mixed with the amendments. The cleaning procedure is detailed in Beryani et al (2022). The following chemicals were used: copper sulphate pentahydrate $CuSO_4*5H_2O$ (Scharlab, Spain, purity > 99.5%), dicamba (Alfa Chemistry, US, purity > 99.5%), citric acid (Chem Lab, Belgium, purity > 99.5%), trisodium citrate dehydrate (Supelco, ACS grade), Zincon (Alfa Aesar), HCl (Merck EMSURE, ACS grade) and NaOH (Honeywell Fluka, ACS grade).

Characterization of the amendments and amendment-sand mixtures

Zeolite and biochar samples were hand-crushed in a ceramic mortar prior use and sieved to discard the fraction larger than 2mm. Corncob was not further milled since already provided in adequate size by the producer. Particle size distribution (PSD) was measured via dry sieving for all samples. Particle shape and elemental chemical composition were investigated using SEM-EDS microscopy (JEOL, Japan). To this aim, air-dried samples were deposited on a stub using carbon (zeolite) or aluminium (biochar and corncob) tape, to avoid interferences of the tape composition with EDS elemental peaks. Powder X-Ray diffraction (Rigaku SmartLab SE) was performed on grounded samples using a CuKα radiation source (λ = 1.54 Å) operating at 40 kV and 30 Ma with scan range 5°-90° and scan step of 0.01°. Particle density was determined applying a modified liquid pycnometer (BLAUBRAND, type Gay-Lussac, volume of 50cm^3, calibrated according to DIN ISO3507) method proposed by Heiskanen (Heiskanen, 1992).

The three amendments where then added separately to the sand at different application rates (1–2–5–10–20% mass fraction) and hand-mixed up to complete homogenization. Bulk density, water holding capacity, pH and salt content of pure amendments, pure sand and of the mixtures were determined according to the European Biochar Certificate (EBC) guidelines for sustainable biochar production (Schmidt, 2015). Further details are provided in paragraph 1 in Supporting Information.

Batch adsorption tests

Adsorption tests were performed in 50 ml sealed glass vials, prepared by adding 2.5 g of solid material (pure sand, pure amendment or a mixture of the two) to 25 ml of pesticide solution ranging 124 to 624 mg/l for copper sulphate and 250 to 1500 mg/l for dicamba, corresponding to the application ranges commonly used in agriculture for the two compounds. For each pesticide, six different initial concentrations were tested in the respective range. The vials were continuously mixed with an overhead shaker (Rotax 6.8, Velp Scientifica, Italy) at 15 rpm for 24 hours to ensure equilibrium between liquid and solid phases. The contact time was

selected based on kinetic adsorption tests, performed using the same experimental procedure at the maximum concentration of the two pesticides in contact with the pure amendments (results reported in paragraph 2 in Supporting Information). After 24 h, the samples were centrifuged at 6000 rpm for 20 mins (Neya 16 centrifuge, REMI, India) and filtered with a PTFE syringe filter with 0.45 μm mesh to remove suspended colloids. The supernatants were then analysed for residual copper or dicamba concentrations: a colorimetric method, described in paragraph 3 in Supporting Information, was adapted from Ghasemi et al. (2003) for copper, while dicamba was directly measured with Uv-VIS spectrophotometer (Specord S600, Analytic Jena, Germany) at 280.5 nm (Figure S3-3). Given the concentration in liquid phase and the liquid volume, the concentration in solid phase was calculated through mass balance.

The experimental results were modelled with Freundlich and Langmuir isotherms. The Freundlich model, suitable for adsorption on heterogeneous surfaces (Vadivelan and Kumar, 2005), was expressed as

$$s_{eq} = K_f {C_e}^{1/n} \quad \text{(eq. 1)}$$

where s_{eq} is the adsorbed concentration [-] in equilibrium with the liquid concentration C_e [ML^{-3}], K_f is the adsorption capacity [$M^{-1/n}L^{3/n}$] and $1/n$ is the Freundlich constant [-], being $1/n < 0.1$ for strongly favourable adsorption, $0.1 < 1/n < 0.5$ for favourable adsorption, $1/n > 0.5$ for unfavourable adsorption.

The Langmuir model, suitable to describe monolayer adsorption (Liu, 2006), was expressed as

$$s_{eq} = \frac{q_{max} L C_e}{1 + L C_e} \quad \text{(eq. 2)}$$

where q_{max} is the maximum adsorption capacity [-] and L the Langmuir adsorption coefficient [L^3M^{-1}].

In order to shade further light on adsorption mechanisms, the zeta potential of biochar, zeolite and corncob diluted to 1 g/l in 3 mM NaCl solution was measured at varying pH (modified by dropwise addition of 50 mM HCl or NaOH) using Dynamic Light Scattering (Malvern, Zetasizer NANO ZSP).

Column leaching tests

Copper and dicamba leaching tests were performed in glass columns (inner diameter 4.1 cm) packed with 320 g of dry sand or of a sand-amendment mixture at 5% application rate. For the mixtures, 16 g of water were added prior packing to allow a slight cohesion between sand and amendment, thus avoiding layering of the two materials during column filling. Column preparation included the following steps: (i) the wet mixture was introduced in small amounts (~20 g) and compacted with a pestle layer by layer; (ii) upward flow (0.2 ml/min) was established until complete saturation; (iii) the column length (~18 cm) was measured, and the column weighted for saturated water content determination. The columns were then left draining by gravity until field capacity was reached. Unsaturated downward flow (0.4 ml/min, corresponding to an infiltration rate of 0.028 cm/min) was then established. A tracer test was performed injecting KBr at constant concentration and the breakthrough electrical conductivity curve was recorded. The unsaturated water content, unsaturated pore volume (PV) time, saturated hydraulic conductivity, and dispersivity were determined via least-squares fitting of the breakthrough curve (BTC) to the classical advection-dispersion equation in unsaturated porous media (paragraph 4 in SI) using Hydrus 1D (Simunek et al., 2013).

After the tracer test, a copper sulphate or dicamba solution (depending on the test) was injected for at least 7.5 h at constant concentration of 624 mg/l or 1500 mg/l, respectively, followed by a flushing with deionized water for 7.5 h. The column outflow was collected using a fraction collector and samples analysed for copper and dicamba with the same methods used for adsorption tests.

At the end of the tests, the columns were extruded and dissected to determine copper and dicamba profiles. Copper was extracted from the solid by using a modified version of the sequential extraction method proposed by Silveira (Silveira et al., 2006), including the following steps: (i) addition of 0.1 M $CaCl_2$ and mixing for 24h to promote ion exchange, (ii) addition of 1M NaOAc (Carlo Erba, purity > 99%) and mixing for 5h for the extraction of Cu(II) adsorbed on grain surface, and (iii) addition of NaOCl (Carlo Erba, solution at 30%) at 90°C for 2h to promote release from the organic matter. Cu precipitated in oxide/hydroxide form is expected not to be recovered. Dicamba was extracted in one step using acetonitrile:$CaCl_2$ 10 mM 70:30 w/w with continuous mixing for 24h. All suspensions were centrifuged at 6000 rpm for 20 min before the analysis.

Copper and dicamba BTCs were modelled with Hydrus 1D (Simunek et al., 2012) using a two-site adsorption equilibrium model, having one site characterized by instantaneous adsorption (eq. 4) and the other one by kinetic adsorption (eq. 5 and 6):

$$\frac{\partial \theta c}{\partial t} + \rho \frac{\partial s^e}{\partial t} + \rho \frac{\partial s^k}{\partial t} = \frac{\partial}{\partial z}\left(\theta D \rho \frac{\partial c}{\partial z}\right) - \frac{\partial qc}{\partial z} - \varphi \quad \text{(eq. 3)}$$

$$s^e = f_e F(c) \quad \text{(eq. 4)}$$

$$\rho \frac{\partial s^k}{\partial t} = \alpha_k \rho \left(s_e^k - s^k\right) - \varphi_k \quad \text{(eq. 5)}$$

$$s_e^k = (1 - f_e) K_d c \quad \text{(eq. 6)}$$

where s^e is the solute concentration adsorbed on the instantaneous (equilibrium) adsorption site expressed as mass of adsorbed solute per unit mass of solid [-], $F(c)$ is the corresponding adsorption isotherm (linear, Langmuir, etc.), f_e is the fraction of exchangeable sites in equilibrium with the liquid phase [-], s^k is the concentration adsorbed on the kinetic (non-equilibrium) adsorption site [-] and s_e^k is the corresponding adsorbed concentration at equilibrium for the kinetic adsorption site -] expressed by the linear isotherm of eq. 6, α_k is the first order rate constant of the kinetic site [T^{-1}], K_d is the partition coefficient for the kinetic site [L^3M^{-1}], φ and φ_k are the sink/source terms accounting for generic reactions [$ML^{-3}T^{-1}$]. The total adsorbed concentration is $s = s^e + s^k$.

Results and discussion

Characterization of the amendments and amendment-sand mixtures

The milled biochar showed a highly heterogeneous morphology (Figure 1a), with larger particles exhibiting a highly intra-porous structure, and smaller ones characterized by an elongated, flat shape. The PSD analysis indicated d_{10}, d_{50} and d_{90} equal to 0.15, 0.7 and 1.9 mm respectively (Figure S5-1). The XRD pattern (Figure 1b) showed the typical biochar composition, including mainly aromatic hydrocarbons and graphite-like carbon structures (Gao et al., 2020). The humped trend in the region 15°<$\theta/2\theta$ < 30° is due to the amorphous

carbonaceous structure resulting from pinewood pyrolysis. The high peak at 26.5° can be associated with pyrolysis of inorganic impurities, mainly graphite (Mohan et al., 2018), while additional peaks at 29°, 36°, 39°, 44° and 48° can be associated with superficial Ca-based compounds such as $CaCO_3$ and CaO (Tran et al., 2015; Waqas et al., 2021).

Hand-milled zeolite showed a distinctly cubic shape, with well-defined angles and smoothed faces due to mechanical crushing (Figure 1c), and particle size lower than 1 mm (d_{10}, d_{50} and d_{90} respectively equal to 0.07, 0.4 and 0.9 mm, Figure S5-2). The XRD pattern (Figure 1d) was consistent with that of Ca-chabazite type zeolite, characterized by a stronger diffraction response at $\theta/2\theta$<15° compared to K-chabazite, as reported by previous crystallographic studies (Leyva-Ramos et al., 2008). This is confirmed by EDS results (Figure S5-4), reporting the presence of Ca (3.2% on average). Peaks in the XRD spectrum other than those characteristic of chabazite were identified at $\theta/2\theta$ = 23.3° - 30.4°. A good agreement was found with sanidine at 23.3°, 27.5°, 27.9° and 29.7°, with illite at 29.9° and 34.14° and with augite at 27.5°, 39.7°, 30.4° and 35.5°, coherently with the nominal sample composition and with previous studies (Ramos et al., 2015).

Corncob (not further milled) showed a higher heterogeneity and irregularity in terms of both PSD (d_{10}, d_{50} and d_{90} equal to 0.2, 0.55 and 0.85 mm, Figure S5-3) and morphology compared to biochar and zeolite. The SEM analysis (Figure 1e) identified the presence of elongated particles interspersed with more compact, jagged ones. The first ones could be attributed to the central pitch part of corncob, the latter to the external glume and wood ring. The XRD pattern (Figure 1f) denoted a highly amorphous lignocellulose material (in particular alfacellulose) identified by two peaks at $\theta/2\theta$ = 16° and 22° (Menezes et al., 2017). Crystalline peaks at 36° and 44° could be traced back to Ca-containing impurities on corncob surface.

Figure 2 reports the results of the sand-amendment mixture characterization (bulk density, water holding capacity, electrical conductivity and pH) obtained following the EBC guidelines for sustainable biochar production. The grain density, measured with a liquid pycnometer, resulted in the following trend: sand (2.6 g/cm^3) > zeolite (2.35 g/cm^3) > biochar (1.6 g/cm^3) > corncob (1.52 g/cm^3). The amendment addition to the sand significantly affected the bulk density of columns dry-packed with the mixtures (Figure 2a), which

decreased linearly from 1.53 g/cm^3 for pure sand with increasing amendment application ratio, reaching 1.33, 1.07 and 0.81 g/cm^3 for 20% application rates of zeolite, corncob and biochar, respectively. The highest bulk density reduction (45.3%) was obtained with biochar, even though the lowest grain density was measured for corncob, suggesting that the bulk density of the mixtures was not a mere weighted mean of the densities of sand and amendment but, rather, was significantly affected by the amendment particle shape. The theoretical porosity corresponding to the measured bulk density (Figure S5-5) increased from 0.41 for pure sand to 0.48, 0.52 and 0.66 for zeolite, corncob and biochar, respectively, at 20% application rate, thus confirming the beneficial effect of amendments (and in particular of biochar and corncob) in terms of reduced bulk density and increased porosity, and consequently reduced soil compaction, higher aeration and potentially lower risk for soil erosion.

The water holding capacity (WHC) increased with increasing the amendment application rates (Figure 2b), and the general observed WHC trend was corncob>biochar>zeolite. At the highest application rates (20%), WHC of 0.34, 0.54 and 0.55 g/g were measured respectively for zeolite-, corncob- and biochar-sand mixtures, corresponding to a WHC increase of 72%, 172% and 177% compared to pure sand. For biochar, both intra-porosity, inter-porosity and the highly irregular surface morphology are expected to have positively affected the biochar-sand mixture WHC (Liu et al., 2017; Verheijen et al., 2019). Similar considerations could be drawn for corncob-sand mixtures, even though no previous literature is available on the characterization of unprocessed corncob as soil amendment. Conversely, the (limited) effect of zeolite on the WHC of the mixtures is mainly attributable to a decrease in particle size, and consequently increase in capillary water retention (Ibrahim and Alghamdi, 2021).

The water electrical conductivity of the pure amendments in contact with water was equal to 29, 165 and 1015 µS/cm for zeolite, biochar and corncob, respectively. The conductivity of the amendment-sand mixtures increased significantly with increasing the amendment application rates, except for zeolite-containing samples, which did not show any significant trend (Figure 2c). Conversely, the high conductivity of pure biochar and corncob denoted a high propensity to free and exchange ions in solution. It is worth to mention that higher values of conductivity, and so salt content, could lead both to a higher potential for ions exchange

and ionic species adsorption, but also to a reduced germinability and damage to crop due to induced salt stress (Buss et al., 2016).

The pH value of the pure materials in contact with water was 7.5, 8.4, 6.7 and 4.7 for sand, biochar, zeolite and corncob, respectively. Coherently, the mixtures showed slightly alkaline pH for biochar, nearly neutral for zeolite and acidic for corncob (Figure 2d). The biochar-sand mixture pH was close to pure biochar pH at all application rates, suggesting that biochar is able to buffer sand, contrary to corncob and zeolite, which showed decreasing pH with increasing application rates.

Adsorption tests

Copper sulphate

The copper sulphate adsorption isotherms for the mixtures are reported in Figure 3a-c as adsorbed concentration s_{eq} (i.e. adsorbed $CuSO_4$ mass over the total mass of adsorbent, i.e. sand + amendment) against $CuSO_4$ residual concentration in liquid phase at equilibrium. Adsorption on pure sand was minimal compared to the mixtures. The adsorption capacity followed the trend biochar>zeolite>corncob. Biochar isotherms showed a trend toward saturation (Figure 3a) for application rates lower than 5%. For rates higher than 10% the same trend can be hypothesized, even though the plateau was not reached since the tests were performed exploring the environmentally-relevant range of $CuSO_4$ concentrations. A similar saturative trend was shown by zeolite-sand mixtures (Figure 3b) but not by corncob-amended sand (Figure 3c).

The experimental isotherms were least-squares fitted to the Langmuir and Freundlich models. The model parameters are reported in Supporting Information in Table S6-1 and their trends as a function of the amendment application rates are reported in Figure 4. As a general rule, both models resulted in very high R^2 values for most isotherms, with a few exceptions. A slightly better fitting with the Langmuir model compared to Freundlich (see R^2 values) suggests a monolayer adsorption mechanism on a homogeneous adsorbent surface, coherently with other studies on $CuSO_4$ interaction with various adsorbents (Wang et al., 2012; Zand and Abyaneh, 2020).

Biochar showed a general better fitting with the Langmuir model compared to the Freundlich one, particularly for rates<20%. Adsorption was unfavourable (1/n≥0.5) for biochar rates≥20%, and favourable (1/n<0.5) for rates<10% (Figure 4a). Conversely, the Freundlich adsorption coefficient K_f showed a bimodal trend in the range 0.09 to 0.74 g $l^{1/n}$ with a peak at application rate of 5% (Figure 4b). Increasing q_{max} with increasing application rate was also observed (Figure 4c). Zeolite showed a very good fitting for both Freundlich and Langmuir isotherms for application rates from 1% to 20%, with slightly higher R^2 values for the Freundlich model at medium-to-high application rates, and particularly for rates>5%. The fitted values of 1/n increased with increasing application rates in the range 0.15-0.3, thus suggesting that copper adsorption on zeolite is a favourable process (Figure 4a). As for corncob, the Langmuir model showed a general better fitting compared to the Freundlich one, with saturation concentration q_{max} significantly lower than those obtained for biochar (Figure 4c).

To further investigate the adsorption capacity and mechanisms, the isotherms were reported also in terms of adsorbed $CuSO_4$ normalized to the mass of amendment (i.e. excluding sand), $s_{eq,norm}$, calculated as

$$s_{eq,norm} = \frac{s_{eq} - s_{eq,AR=0\%}(1 - AR)}{AR}$$

where $s_{eq,AR=0\%}$ is the adsorbed concentration measured in the absence of amendment (i.e. when sand is the only solid in the batch). An unexpected trend of the results was obtained (Figures 3d-f): with decreasing application rates, $s_{eq,norm}$increased for all tested materials. This suggests that adsorption is more efficient in the presence of a low adsorbent content in the solid fraction, even though the adsorption on sand grains is minimal.

In general, the main expected mechanisms of $CuSO_4$ removal from water include surface adsorption (due to electrostatic attraction and ion exchange), and precipitation of Cu oxides and hydroxides at favourable hydrochemical conditions (Tan et al., 2015; Zhao et al., 2020). For both mechanisms, pH plays a key role. The pH was acidic in all our tests due to the presence of $CuSO_4$ in solution, and was slightly affected by the amendment application rates (Figure S6-1): in particular, pH was close to 5 for pure sand and increased with increasing both zeolite and biochar application rate toward plateau values of approximately 6 and 7,

311 respectively, but decreased toward approximately 4.5 for corncob-sand mixtures (coherently with the more
312 acidic pH of corncob). Concerning copper precipitation, Jiang at al. (Jiang et al., 2016) indicate that, for acidic
313 $CuSO_4$ solutions in contact with biochar, the formation of insoluble $Cu(OH)_2$ is expected starting from pH
314 above 6. Thus, the pH values of our tests would explain the limited Cu removal observed for pure sand and
315 corncob (Figure 3f), and the higher one for zeolite and biochar (Figures 3d and 3e), even though the pH values
316 measured for zeolite- and biochar-sand mixtures are not high enough to suggest a predominance of
317 precipitation as removal mechanism. The pH influences the surface charge of the adsorbent and thus the
318 surface adsorption due to electrostatic attraction toward dissolved copper ions. Zeta potential, which can be
319 used as an indirect measurement of surface charge, was negative for all amendments in our tests (Figure S5-
320 6), and decreased with increasing pH, suggesting a higher affinity of the amendments to the copper cations
321 at higher pH. Again this trend would explain the corncob isotherms but not those obtained for zeolite and
322 biochar. Consequently, other properties controlling surface adsorption are likely to play the major role in our
323 tests. Among them, the specific surface area of the amendment is likely the parameter controlling adsorption
324 capacity. It was observed that during the adsorption experiments the particle size of the amendment was
325 reduced: optical microscope analysis of corncob particles before and after the adsorption tests evidenced a
326 clear decrease in size (Figure S6-2 in Supporting Information); particle size distributions obtained via image
327 processing (ImageJ, National Institutes of Health, US) showed that the difference is more pronounced at low
328 application rate (5%) and negligible at the highest application rate (20%) (Figure S6-3). This can be explained
329 by sand acting as ball milling, thus reducing amendment particle size during mixing with the overhead shaker
330 (Shan et al., 2016): the higher the sand content in the sample, the more effective the milling. Higher copper
331 loading potential at decreasing particle size was also reported previously for biochar, and was attributed to
332 a larger surface area available and easier accessibility to pores for finer adsorbents (Zou et al., 2006).

333

334 ***Dicamba***

335 The dicamba adsorption isotherms (Figure 5) show a higher overall adsorption capacity for corncob
336 and biochar, followed by zeolite. For all tested materials, the removal efficiency increased with increasing

337 application rate, similarly to what observed for $CuSO_4$. The contribution of sand to dicamba adsorption is
338 minor, even though not negligible, compared to the three amendments (see black dotted isotherms in Figure
339 5). For biochar- and corncob-sand mixtures (Figures 5a and 5c), the isotherms showed an asymptotic trend
340 toward a saturation concentration for rates<10% and <5%, respectively. The saturative trend is further
341 evidenced when the isotherms are normalized to the mass of amendment (Figure 5d and f). Conversely,
342 zeolite isotherms were distinctly linear at all tested application rates, without any evident saturative
343 behaviour (Figures 5b and e). It is worth observing that the removal efficiency of pure zeolite is lower than
344 the other two pure amendments, but for low application rates (up to 2%) the removal efficiency of zeolite-
345 sand mixtures (Figure 5b) was comparable to or higher than the others. This is reflected by remarkably higher
346 normalized isotherms for zeolite at low application rates (Figure 5e).

347 The overall increasing adsorption efficiency of the adsorbents with decreasing application rates, as
348 evidenced in Figures 5d-f, is in line with the results obtained for $CuSO_4$, and confirms the key role of sand-
349 mediated milling of the amendments in increasing the sorption efficiency in batch tests. However, the effect
350 of comminution alone is not sufficient to explain all the results reported in Figures 5d-f, and in particular the
351 overall reduced adsorption efficiency of biochar compared to corncob and zeolite. A key role in this sense is
352 likely played by pH: dicamba in solution exhibits an acidic behaviour (Azejjel et al., 2008), with pKa equal to
353 1.98 (Carrizosa et al., 2001). The dissociated dicamba molecule assumes a negative charge, that contrasts
354 with the negative surface charge of zeolite/biochar/corncob. Thus, the dicamba adsorption is favoured when
355 the compound is present in its molecular form, rather than when dissociated, and consequently at strongly
356 acidic pH. Figure S6-4 in Supporting Information reports the trends for the pH measured in batch tests as a
357 function of amendment application rates. For pure sand, the sample pH was 2.8, close to pKa. For all
358 amendments, the pH increased with increasing application rate. As for biochar, pH rapidly approached
359 neutrality for application rates higher than 5%, corresponding to a predominantly dissociated form of
360 dicamba and thus to a lower affinity of the molecule to the amendment. Correspondingly, biochar exhibited
361 the lowest normalized isotherms among the three tested materials (Figure 5d). For zeolite and corncob, the
362 pH remained close to 3 for application rates lower than 5%. Correspondingly, the normalized isotherms of

Figures 5e and f showed higher adsorbed concentrations at low application rates compared to biochar. This finding suggests that, along with the optimal adsorbent milling obtained at low application rates, also pH played a fundamental role in controlling dicamba adsorption potential.

The modelling of dicamba isotherms with Langmuir and Freundlich equations (coefficients in Table S6-2 in Supporting Information, trends with application rates in Figure 6) showed a good fitting for both models and for all the three materials, with slightly higher R^2 values for the Langmuir model. For all zeolite-sand mixtures, linear adsorption was confirmed, being always 1/n>1 (Figure 6a). The Freundlich adsorption coefficient K_f slightly decreased for biochar- and corncob-sand mixtures, and increased for zeolite-sand mixtures, with increasing application rate (Figure 6b). Corncob and biochar showed 1/n<1, increasing toward the unit with increasing application rates, thus suggesting adsorption of pseudo-linear type.

Leaching tests

Column hydrodynamic characterization

The hydrodynamic parameters of the columns in leaching tests in unsaturated conditions are reported in Table 1. A higher water content θ for the biochar-sand column compared to others was expected according to the higher amendment WHC, higher biochar porosity and heterogeneous particle structure. The saturated hydraulic conductivity K_s was higher for pure sand and decreased progressively for corncob-, zeolite-, and biochar-sand mixtures, in accordance with previous literature (Sarabi and Sepaskhah, 2012; Yan et al., 2021). Conversely, the hydrodynamic dispersivity α was similar in all tests.

Copper sulphate leaching tests

Figure 7a reports the breakthrough curves of copper sulphate in the four columns as a function of the injected unsaturated pore volumes (PVs). In general, the ability of the amendment-sand mixture to retain $CuSO_4$ followed the order sand < corncob-sand < zeolite-sand / biochar-sand mixtures. In pure sand, a relevant delay

387 in the breakthrough of $CuSO_4$ was observed, with $C/C_0>0$ after 1.5 PVs, suggesting the occurrence of
388 reversible equilibrium adsorption. A fairy constant concentration $C/C_0 \sim 0.9$ was then measured for the entire
389 duration of the injection step, indicating the occurrence, in parallel, of reversible equilibrium adsorption and
390 kinetic irreversible adsorption or of precipitation. For zeolite and biochar, an almost null breakthrough was
391 observed, with no $CuSO_4$ release even during post-flushing with deionized water, thus suggesting that $CuSO_4$
392 was irreversibly adsorbed and/or precipitated in the tested hydrochemical conditions. Negligible
393 breakthrough was observed also for the sand-corncob column for 4.5 PVs, followed by a limited
394 breakthrough. However, during flushing a significant desorption occurred, indicating in this case a weaker
395 and partly reversible interaction between Cu and corncob.

396 Relevant additional information can be obtained from the profiles of retained concentration of $CuSO_4$,
397 obtained dissecting the columns at the end of the leaching tests (Figure 7b). An almost constant copper
398 concentration was detected along the vertical direction in pure sand (~0.09 mg/g) and for the corncob-sand
399 mixture (~0.29 mg/g, except for the deepest 4 cm). It is worth noticing that in both tests a non-negligible
400 copper breakthrough concentration was measured at the end of injection, thus suggesting the two columns
401 reached saturation along the entire column (for sand) or at least in its upper part (for the corncob-sand
402 mixture). Conversely, a different profile shape was observed for zeolite- and biochar-sand mixtures: in both
403 cases, a higher Cu concentration was retained in the first 6 cm and negligible concentrations in the deepest
404 part of the column, thus suggesting that biochar and zeolite have a much higher sorption capacity and column
405 saturation was not reached during the test.

406 A closer analysis of the percentage of Cu recovered in each step of the sequential extraction method (aimed
407 at recovering Cu aliquots retained due to different phenomena) provides additional information on the
408 retention mechanisms (Figure S7-1 in Supporting Information). In all tests, the highest recovery was obtained
409 in the first extraction step, aimed at promoting Cu(II) release via ion exchange. This predominance is
410 particularly evident for corncob and biochar, confirming the higher ion exchange capacity of these
411 amendments compared to pure sand and zeolite. For the second extraction, aimed at releasing Cu adsorbed
412 on mineral surfaces, the highest recovery was obtained for pure sand, followed by zeolite-, biochar- and

corncob-sand mixtures, indicating a slightly higher affinity of Cu to sand compared to zeolite surface. In the third extraction, aimed at extracting Cu adsorbed on the organic matter, the largest recovery percentage, as expected, was obtained for corncob. In all tests, and particularly for zeolite- and biochar-sand mixtures, a non-negligible fraction of Cu (Table 1) was not recovered at column outflow nor in the extraction procedure, suggesting that Cu precipitation in the form of oxides/hydroxides (which cannot be extracted by none of the methods adopted in the three steps) also partly occurred.

The breakthrough curve for pure sand was modelled using eq. 3 - 6 with one instantaneous (equilibrium) adsorption site (eq. 4) following a Langmuir isotherm, and one kinetic adsorption site (eq. 5). The fitting was satisfactory (Figure S7-2) with R^2 = 0.91. For the equilibrium site, the Langmuir parameters obtained were q_{max} = 4.02·10^{-1} mg/g and L = 1.66·10^{-3} l/mg, similar to the values obtained in batch tests for $CuSO_4$ adsorption onto pure sand (Table S6-1). As for the kinetic site, α_k = 1.29·10^{-3} min^{-1} and φ_k = 2.37·10^{-3} min^{-1} were obtained. The fraction of instantaneous adsorption sites where adsorption f_e was equal to 0.42, in agreement with the similar percentages of Cu recovery obtained in the first and second steps of the sequential extraction method.

Dicamba

Contrary to $CuSO_4$ leaching tests, dicamba showed a significant breakthrough in all tested columns, corresponding to an overall lower affinity to the tested amendments (Figure 8a). No evident retardation was observed for pure sand and zeolite-sand mixture, while breakthrough was retarded for biochar- and corncorb-sand mixtures, with a retardation factor equal to 1.8 and 2.5, respectively. Beside retardation, which suggests the occurrence of instantaneous equilibrium adsorption, all breakthrough curves also showed a steady-state concentration plateau lower than the injected one, suggesting the concomitant occurrence of kinetic adsorption. From a qualitative point of view, the affinity of dicamba for the sorbent materials confirmed the same trend corncob>biochar>zeolite evidenced by batch tests, and by mass balances (Table 1).

Figure 8b reports the vertical profile of retained dicamba at the end of the leaching tests. The profile for the corncob-sand mixture was not determined due to interference with other substances released by the corncob matrix. As a general trend, higher adsorption was observed in the upper part of the columns, where higher concentrations in pore water were present, even though concentrations are not negligible also at higher depths. The non-negligible concentrations of adsorbed dicamba measured along the column at the end of the test confirm the presence of two concurrent adsorption mechanisms (instantaneous and kinetic, the second being partly irreversible) hypothesized based on breakthrough curves: if adsorption was totally reversible, no significant retained concentration should have been measured, having breakthrough curves reached negligible values at the end of all tests.

The breakthrough curves of all dicamba leaching tests were modelled assuming the same mechanisms used for $CuSO_4$ (parameter in Table S7-1, modelled curves in Figure S7-3 in Supporting Information). The fitting was visually satisfactory with $R^2>0.95$ for all tests except for the sand-corncob mixture. The first-order rate constant for dissolved phase α_k was higher for sand and sand-zeolite mixtures compared to biochar- and corncob-sand columns, suggesting that the latter materials reach faster equilibrium for the kinetic site compared to biochar- and corncob-sand columns. Comparing batch and column equilibrium adsorption parameters, and in particular the maximum adsorption capacity s_{max} (Figure 9a), it can be observed that in all cases the q_{max} values obtained in batch were higher than those obtained in columns, but with the same trend, likely due to the better and longer contact between adsorbents and dicamba solutions.

Conclusions

In this study, zeolite, biochar and corncob were used to adsorb and reduce the mobility in water and soil of two pesticides, namely copper sulphate and dicamba. These amendments were mixed with silica sand at different application rates. A general decrease in bulk density and a notable increase in water holding capacity were observed with increasing application rates, particularly for biochar and corncob. This suggests their higher potential for enhancing water storage in fields during drought conditions. Conversely, zeolite

showed minimal impact on both bulk density and water holding capacity. The addition of amendments also significantly altered the pH. Thus, the physical and chemical effects of adding amendments to sand or soil in crop fields must be taken carefully into account, particularly in the presence of plants and crops with specific tolerance thresholds to salt/pH/soil humidity.

The ability of the different mixtures to adsorb pesticides were first tested in batch. The amendment initial particle size distribution, application rate and the way of mixing used during adsorption test played crucial roles in the adsorption tests. In particular, head-over-head mixing allowed a significant reduction of amendment particle size due to friction with sand, thus enhancing adsorption rates, particularly at the lowest application rates. This finding evidences the importance of a careful evaluation of the results of batch adsorption tests, particularly when extrapolating their results to larger scales (column or field), due to the high impact of the specific operating conditions on the results. Highly charged amendments, such as biochar and zeolite, showed a higher affinity with copper, while dicamba was highly adsorbed by corncob due to its high organic matter content. The Langmuir adsorption model best fitted the experimental results for both copper sulphate and dicamba, suggesting a monolayer adsorption onto amendment surfaces.

Preliminary column leaching tests were conducted to assess the amendments' effects under hydrodynamic conditions. The results confirmed the higher affinity of biochar and zeolite for copper sulphate, with negligible leaching of copper from the column, compared to sand and sand-corncob columns. For dicamba, higher retardation factor and consequently higher retention were observed in the corncob-sand mixture. In field conditions, this would result in longer retention of dicamba in the top soil, thus making its biodegradation more favourable.

In conclusion, natural soil amendments can be used not only to improve the physical-chemical characteristics of the soil, as currently practiced in some agronomic techniques, but also to enhance adsorption of pesticides in the soil, thus limiting the spreading of both diffuse and local contaminations in agricultural settings. The results of this study also highlight the potential benefits of combining multiple amendments at the field scale,

where diverse types of pesticides are applied, to limit the overall leaching of agrochemicals into deeper soil and groundwater.

Cited literature

Aguiar, A.C.M. de, Silva, E.M.G. da, Barcellos Júnior, L.H., Paula, D.F. de, Souza, P.S.R. de, Guimarães, T., Ovejero, R.F.L., Palhano, M.G., Silva, A.A. da, Mendes, K.F., 2023. Sorption, leaching, and degradation of dicamba in two Brazilian soils: A study into soil layers. Crop Protection 174, 106393. https://doi.org/10.1016/j.cropro.2023.106393

Ahmad, M., Rajapaksha, A.U., Lim, J.E., Zhang, M., Bolan, N., Mohan, D., Vithanage, M., Lee, S.S., Ok, Y.S., 2014. Biochar as a sorbent for contaminant management in soil and water: A review. Chemosphere 99, 19–33. https://doi.org/10.1016/j.chemosphere.2013.10.071

Aldrich, A.P., Kistler, D., Sigg, L., 2002. Speciation of Cu and Zn in Drainage Water from Agricultural Soils. Environmental Science & Technology 36, 4824–4830. https://doi.org/10.1021/es025813x

Azejjel, H., Aatouf, N., Draoui, K., Rodriguez-Cruz, S., Sánchez-Martín, M., 2008. Influence of soil properties on the adsorption of two ionisable herbicides by Moroccan soils. Fresenius Environmental Bulletin 17, 1627–1633.

Bakshi, S., He, Z.L., Harris, W.G., 2014. Biochar Amendment Affects Leaching Potential of Copper and Nutrient Release Behavior in Contaminated Sandy Soils. Journal of Environmental Quality 43, 1894–1902. https://doi.org/10.2134/jeq2014.05.0213

Beryani, A., Bianco, C., Casasso, A., Sethi, R., Tosco, T., 2022. Exploring the potential of graphene oxide nanosheets for porous media decontamination from cationic dyes. Journal of Hazardous Materials 424, 127468. https://doi.org/10.1016/j.jhazmat.2021.127468

Buss, W., Graham, M.C., Shepherd, J.G., Mašek, O., 2016. Suitability of marginal biomass-derived biochars for soil amendment. Science of The Total Environment 547, 314–322. https://doi.org/10.1016/j.scitotenv.2015.11.148

Cao, X., Ma, L., Liang, Y., Gao, B., Harris, W., 2011. Simultaneous immobilization of lead and atrazine in contaminated soils using dairy-manure biochar. Environ Sci Technol 45, 4884–4889. https://doi.org/10.1021/es103752u

Carrizosa, M.J., Koskinen, W.C., Hermosin, M.C., Cornejo, J., 2001. Dicamba adsorption–desorption on organoclays. Applied Clay Science 18, 223–231. https://doi.org/10.1016/S0169-1317(01)00037-0

Cataldo, E., Salvi, L., Paoli, F., Fucile, M., Masciandaro, G., Manzi, D., Masini, C.M., Mattii, G.B., 2021. Application of Zeolites in Agriculture and Other Potential Uses: A Review. Agronomy 11, 1547.

Diacono, M., Montemurro, F., 2010. Long-term effects of organic amendments on soil fertility. A review. Agronomy for Sustainable Development 30, 401–422. https://doi.org/10.1051/agro/2009040

Dordio, A., Carvalho, A.J., 2013. Constructed wetlands with light expanded clay aggregates for agricultural wastewater treatment. The Science of the total environment 463–464, 454–61. https://doi.org/10.1016/j.scitotenv.2013.06.052

Ferretti, G., Keiblinger, K.M., Faccini, B., Di Giuseppe, D., Mentler, A., Zechmeister-Boltenstern, S., Coltorti, M., 2020. Effects of Different Chabazite Zeolite Amendments to Sorption of Nitrification Inhibitor 3,4-Dimethylpyrazole Phosphate (DMPP) in Soil. Journal of Soil Science and Plant Nutrition 20, 973–978. https://doi.org/10.1007/s42729-020-00184-3

Gao, Y., Xiao, Y., Mao, K., Qin, X., Zhang, Yuan, Li, D., Zhang, Yanhui, Li, J., Wan, H., He, S., 2020. Thermoresponsive polymer-encapsulated hollow mesoporous silica nanoparticles and their application in insecticide delivery. Chemical Engineering Journal 383, 123169. https://doi.org/10.1016/j.cej.2019.123169

Ghasemi, J., Ahmadi, S., Torkestani, K., 2003. Simultaneous determination of copper, nickel, cobalt and zinc using zincon as a metallochromic indicator with partial least squares. Analytica Chimica Acta 487, 181–188. https://doi.org/10.1016/s0003-2670(03)00556-7

534 Ghosh, U., Luthy, R.G., Cornelissen, G., Werner, D., Menzie, C.A., 2011. In-situ Sorbent Amendments: A New
535 Direction in Contaminated Sediment Management. Environ. Sci. Technol. 45, 1163–1168.
536 https://doi.org/10.1021/es102694h
537 Granetto, M., Serpella, L., Fogliatto, S., Re, L., Bianco, C., Vidotto, F., Tosco, T., 2022. Natural clay and
538 biopolymer-based nanopesticides to control the environmental spread of a soluble herbicide.
539 Science of The Total Environment 806, 151199. https://doi.org/10.1016/j.scitotenv.2021.151199
540 Heiskanen, J., 1992. Comparison of three methods for determining the particle density of soil with liquid
541 pycnometers. Communications in Soil Science and Plant Analysis 23, 841–846.
542 https://doi.org/10.1080/00103629209368633
543 Hoy, J., Swanson, N., Seneff, S., 2015. The High Cost of Pesticides: Human and Animal Diseases. Poultry,
544 Fisheries & Wildlife Sciences 03. https://doi.org/10.4172/2375-446X.1000132
545 Ibrahim, H.M., Alghamdi, A.G., 2021. Effect of the Particle Size of Clinoptilolite Zeolite on Water Content
546 and Soil Water Storage in a Loamy Sand Soil. Water 13. https://doi.org/10.3390/w13050607
547 Jiang, S., Huang, L., Nguyen, T.A.H., Ok, Y.S., Rudolph, V., Yang, H., Zhang, D., 2016. Copper and zinc
548 adsorption by softwood and hardwood biochars under elevated sulphate-induced salinity and
549 acidic pH conditions. Chemosphere 142, 64–71.
550 https://doi.org/10.1016/j.chemosphere.2015.06.079
551 Joshi, V., Srivastava, A., Srivastava, P.C., 2016. Potential of some soil amendments in reducing leaching of
552 fipronil to groundwater. International Journal of Environmental Science and Technology 13, 631–
553 638. https://doi.org/10.1007/s13762-015-0883-1
554 Kookana, R.S., Sarmah, A.K., Van Zwieten, L., Krull, E., Singh, B., 2011. Chapter three - Biochar Application to
555 Soil: Agronomic and Environmental Benefits and Unintended Consequences, in: Sparks, D.L. (Ed.),
556 Advances in Agronomy. Academic Press, pp. 103–143. https://doi.org/10.1016/B978-0-12-385538-
557 1.00003-2
558 Kumari, K.G.I.D., Moldrup, P., Paradelo, M., Elsgaard, L., de Jonge, L.W., 2016. Soil Properties Control
559 Glyphosate Sorption in Soils Amended with Birch Wood Biochar. Water, Air, & Soil Pollution 227,
560 174. https://doi.org/10.1007/s11270-016-2867-2
561 Lahori, A.H., Zhang, Z., Guo, Z., Li, R., Mahar, A., Awasthi, M.K., Wang, P., Shen, F., Kumbhar, F., Sial, T.A.,
562 Zhao, J., Guo, D., 2017. Beneficial effects of tobacco biochar combined with mineral additives on
563 (im)mobilization and (bio)availability of Pb, Cd, Cu and Zn from Pb/Zn smelter contaminated soils.
564 Ecotoxicology and Environmental Safety 145, 528–538.
565 https://doi.org/10.1016/j.ecoenv.2017.07.071
566 Leyva-Ramos, R., Jacobo-Azuara, A., Diaz-Flores, P.E., Guerrero-Coronado, R.M., Mendoza-Barron, J.,
567 Berber-Mendoza, M.S., 2008. Adsorption of chromium(VI) from an aqueous solution on a
568 surfactant-modified zeolite. Colloids and Surfaces A: Physicochemical and Engineering Aspects 330,
569 35–41. https://doi.org/10.1016/j.colsurfa.2008.07.025
570 Liu, G.C., Pan, M.Q., Song, J.Y., Guo, M.Y., Xu, L.N., Xin, Y.J., 2022. Investigating the effects of biochar
571 colloids and nanoparticles on cucumber early seedlings. Sci Total Environ 804.
572 https://doi.org/10.1016/j.scitotenv.2021.150233
573 Liu, Y., 2006. Some consideration on the Langmuir isotherm equation. Colloids and Surfaces A:
574 Physicochemical and Engineering Aspects 274, 34–36.
575 https://doi.org/10.1016/j.colsurfa.2005.08.029
576 Liu, Z., Dugan, B., Masiello, C.A., Gonnermann, H.M., 2017. Biochar particle size, shape, and porosity act
577 together to influence soil water properties. PLOS ONE 12, e0179079.
578 https://doi.org/10.1371/journal.pone.0179079
579 Menezes, D.B., Brazil, O.A.V., Romanholo-Ferreira, L.F., de Lourdes T. M. Polizeli, M., Ruzene, D.S., Silva,
580 D.P., Costa, L.P., Hernández-Macedo, M.L., 2017. Prospecting fungal ligninases using corncob
581 lignocellulosic fractions. Cellulose 24, 4355–4365. https://doi.org/10.1007/s10570-017-1427-2
582 Mohan, D., Abhishek, K., Sarswat, A., Patel, M., Singh, P., Pittman, C.U., 2018. Biochar production and
583 applications in soil fertility and carbon sequestration – a sustainable solution to crop-residue
584 burning in India. RSC Adv. 8, 508–520. https://doi.org/10.1039/C7RA10353K

585 Mondal, M., Biswas, B., Garai, S., Sarkar, S., Banerjee, H., Brahmachari, K., Bandyopadhyay, P.K., Maitra, S.,
586 Brestic, M., Skalicky, M., Ondrisik, P., Hossain, A., 2021. Zeolites Enhance Soil Health, Crop
587 Productivity and Environmental Safety. Agronomy 11. https://doi.org/10.3390/agronomy11030448
588 Ramos, C.G., Querol, X., Oliveira, M.L.S., Pires, K., Kautzmann, R.M., Oliveira, L.F.S., 2015. A preliminary
589 evaluation of volcanic rock powder for application in agriculture as soil a remineralizer. Sci Total
590 Environ 512–513, 371–380. https://doi.org/10.1016/j.scitotenv.2014.12.070
591 Ritter, W.F., 1988. Reducing Impacts of Nonpoint Source Pollution from Agriculture - a Review. J Environ Sci
592 Heal A J Environ Sci Heal A 23, 645–667.
593 Sarabi, S., Sepaskhah, A., 2012. Effect of zeolite and saline water application on saturated hydraulic
594 conductivity and infiltration in different soil textures. Archives of Agronomy and Soil Science 59, 1–
595 12. https://doi.org/10.1080/03650340.2012.675626
596 Schmidt, H.-P., 2015. European Biochar Certificate (EBC) - guidelines version 6.1.
597 https://doi.org/10.13140/RG.2.1.4658.7043
598 Sethi, R., Di Molfetta, A., 2019. GROUNDWATER ENGINEERING A Technical Approach to Hydrogeology,
599 Contaminant Transport and Groundwater Remediation. https://doi.org/10.1007/978-3-030-20516-
600 4
601 Shan, D., Deng, S., Zhao, T., Wang, B., Wang, Y., Huang, J., Yu, G., Winglee, J., Wiesner, M.R., 2016.
602 Preparation of ultrafine magnetic biochar and activated carbon for pharmaceutical adsorption and
603 subsequent degradation by ball milling. Journal of Hazardous Materials 305, 156–163.
604 https://doi.org/10.1016/j.jhazmat.2015.11.047
605 Silveira, M.L., Alleoni, L.R.F., O'Connor, G.A., Chang, A.C., 2006. Heavy metal sequential extraction
606 methods—A modification for tropical soils. Chemosphere 64, 1929–1938.
607 https://doi.org/10.1016/j.chemosphere.2006.01.018
608 Simunek, J., Jacques, D., Langergraber, G., Bradford, S.A., Sejna, M., van Genuchten, M.T., 2013. Numerical
609 Modeling of Contaminant Transport Using HYDRUS and its Specialized Modules. J Indian I Sci 93,
610 265–284.
611 Simunek, J., van Genuchten, M.T., Sejna, M., 2012. Hydrus: Model Use, Calibration, and Validation. T Asabe
612 55, 1261–1274.
613 Sud, D., Mahajan, G., Kaur, M.P., 2008. Agricultural waste material as potential adsorbent for sequestering
614 heavy metal ions from aqueous solutions – A review. Bioresource Technology 99, 6017–6027.
615 https://doi.org/10.1016/j.biortech.2007.11.064
616 Tan, X., Liu, Y., Zeng, G., Wang, X., Hu, X., Gu, Y., Yang, Z., 2015. Application of biochar for the removal of
617 pollutants from aqueous solutions. Chemosphere 125, 70–85.
618 https://doi.org/10.1016/j.chemosphere.2014.12.058
619 Tong, Y., McNamara, P.J., Mayer, B.K., 2019. Adsorption of organic micropollutants onto biochar: a review
620 of relevant kinetics, mechanisms and equilibrium. Environ. Sci.: Water Res. Technol. 5, 821–838.
621 https://doi.org/10.1039/C8EW00938D
622 Tran, H., You, S.-J., Chao, H.-P., 2015. Effect of pyrolysis temperatures and times on the adsorption of
623 cadmium onto orange peel derived biochar. Waste Management & Research 34.
624 https://doi.org/10.1177/0734242X15615698
625 Vadivelan, V., Kumar, K.V., 2005. Equilibrium, kinetics, mechanism, and process design for the sorption of
626 methylene blue onto rice husk. Journal of Colloid and Interface Science 286, 90–100.
627 https://doi.org/10.1016/j.jcis.2005.01.007
628 Verheijen, F.G.A., Zhuravel, A., Silva, F.C., Amaro, A., Ben-Hur, M., Keizer, J.J., 2019. The influence of biochar
629 particle size and concentration on bulk density and maximum water holding capacity of sandy vs
630 sandy loam soil in a column experiment. Geoderma 347, 194–202.
631 https://doi.org/10.1016/j.geoderma.2019.03.044
632 Wang, J., Chen, T., Li, S., Yue, Z.-B., Jin, J., He, G., Zhang, H., 2012. Biosorption of Copper (II) from Aqueous
633 Solutions with Rape Straw. Geomicrobiology Journal 29, 250–254.
634 https://doi.org/10.1080/01490451.2011.598603

Wang, S.Z., Wang, J.L., 2022. Magnetic 2D/2D oxygen doped g-C3N4/biochar composite to activate peroxymonosulfate for degradation of emerging organic pollutants. J Hazard Mater 423. https://doi.org/10.1016/j.jhazmat.2021.127207

Waqas, M., Asam, Z.-Z., Rehan, M., Anwar, M., Khattak, R., Ismail, I., Tabatabaei, M., Nizami, Dr.A.-S., 2021. Development of biomass-derived biochar for agronomic and environmental remediation applications. Biomass Conversion and Biorefinery 11, 1–23. https://doi.org/10.1007/s13399-020-00936-2

Yan, Y., Akbar Nakhli, S.A., Jin, J., Mills, G., Willson, C.S., Legates, D.R., Manahiloh, K.N., Imhoff, P.T., 2021. Predicting the impact of biochar on the saturated hydraulic conductivity of natural and engineered media. Journal of Environmental Management 295, 113143. https://doi.org/10.1016/j.jenvman.2021.113143

Zand, A.D., Abyaneh, M.R., 2020. Adsorption of Lead, manganese, and copper onto biochar in landfill leachate: implication of non-linear regression analysis. Sustainable Environment Research 30, 18. https://doi.org/10.1186/s42834-020-00061-9

Zhao, S., Ta, N., Wang, X., 2020. Absorption of Cu(II) and Zn(II) from Aqueous Solutions onto Biochars Derived from Apple Tree Branches. Energies 13. https://doi.org/10.3390/en13133498

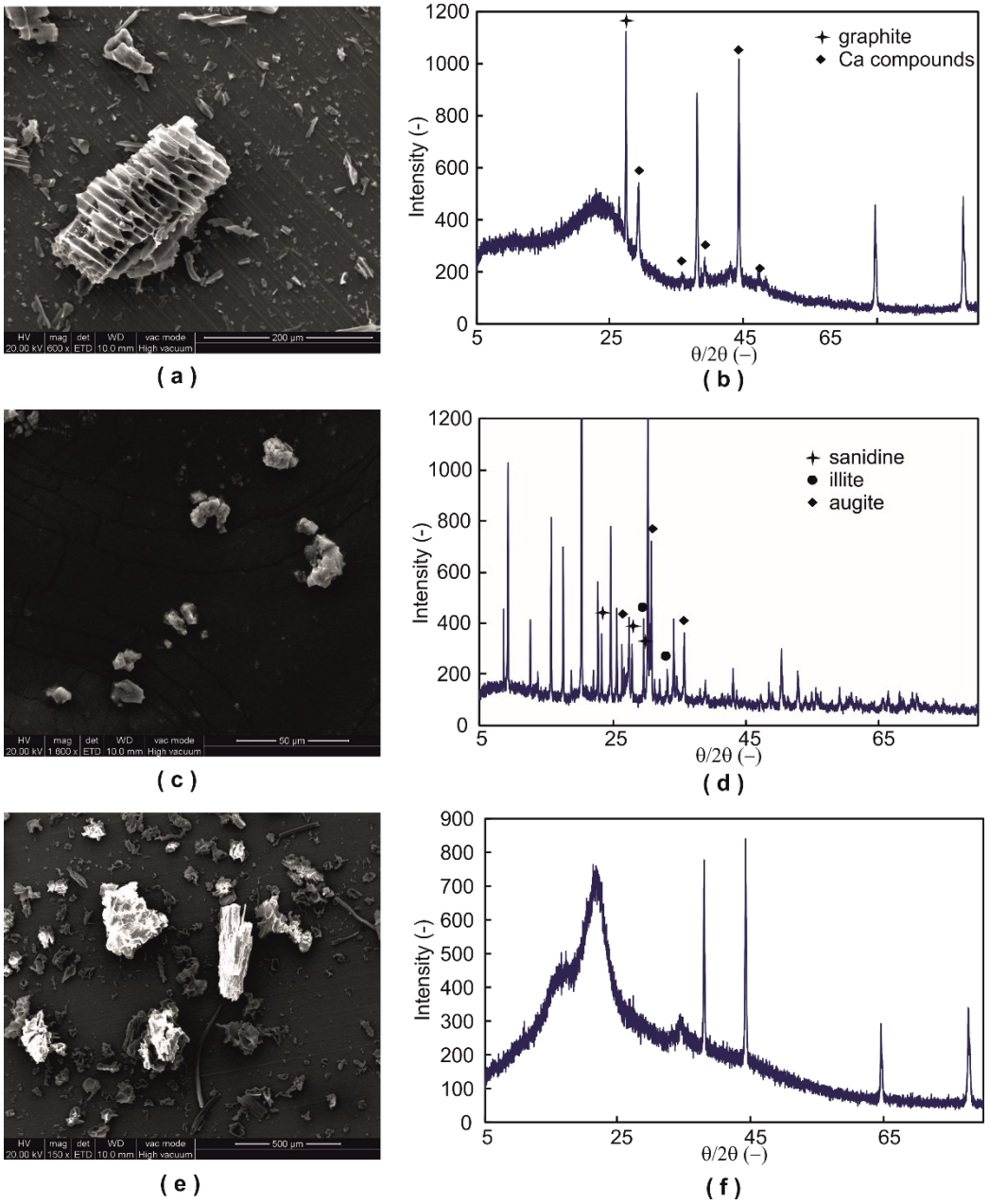
Zou, W., Han, R., Chen, Z., Jinghua, Z., Shi, J., 2006. Kinetic study of adsorption of Cu(II) and Pb(II) from aqueous solutions using manganese oxide coated zeolite in batch mode. Colloids and Surfaces A: Physicochemical and Engineering Aspects 279, 238–246. https://doi.org/10.1016/j.colsurfa.2006.01.008

Acknowledgements

The authors thank prof. Rajandrea Sethi for guidance and support in the study development.

The part of the study concerning corncob has received funding in the framework of the project NODES from the MUR - M4C2 1.5 of PNRR funded by the European Union - NextGenerationEU (Grant agreement no. ECS00000036).

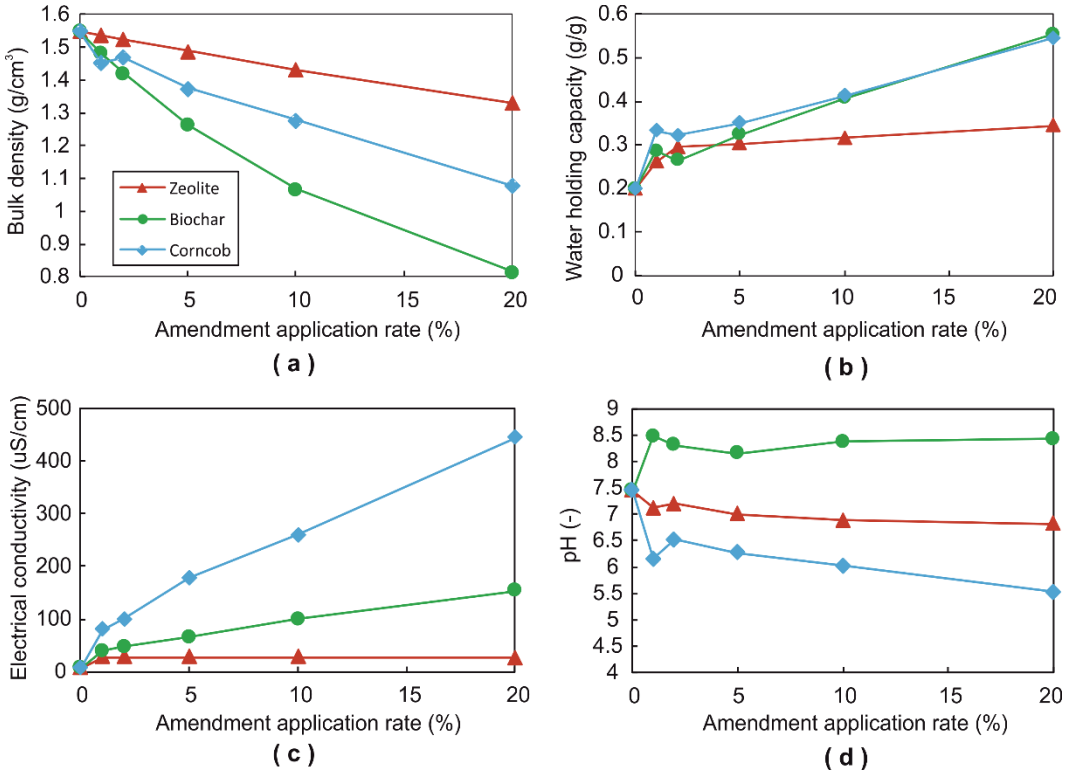
663 **FIGURES**



664

665 *Figure 1 SEM images (a, c, e) and XRD spectra (b, d, f) for biochar (a, b), zeolite (c, d) and corncob (e,f) samples.*

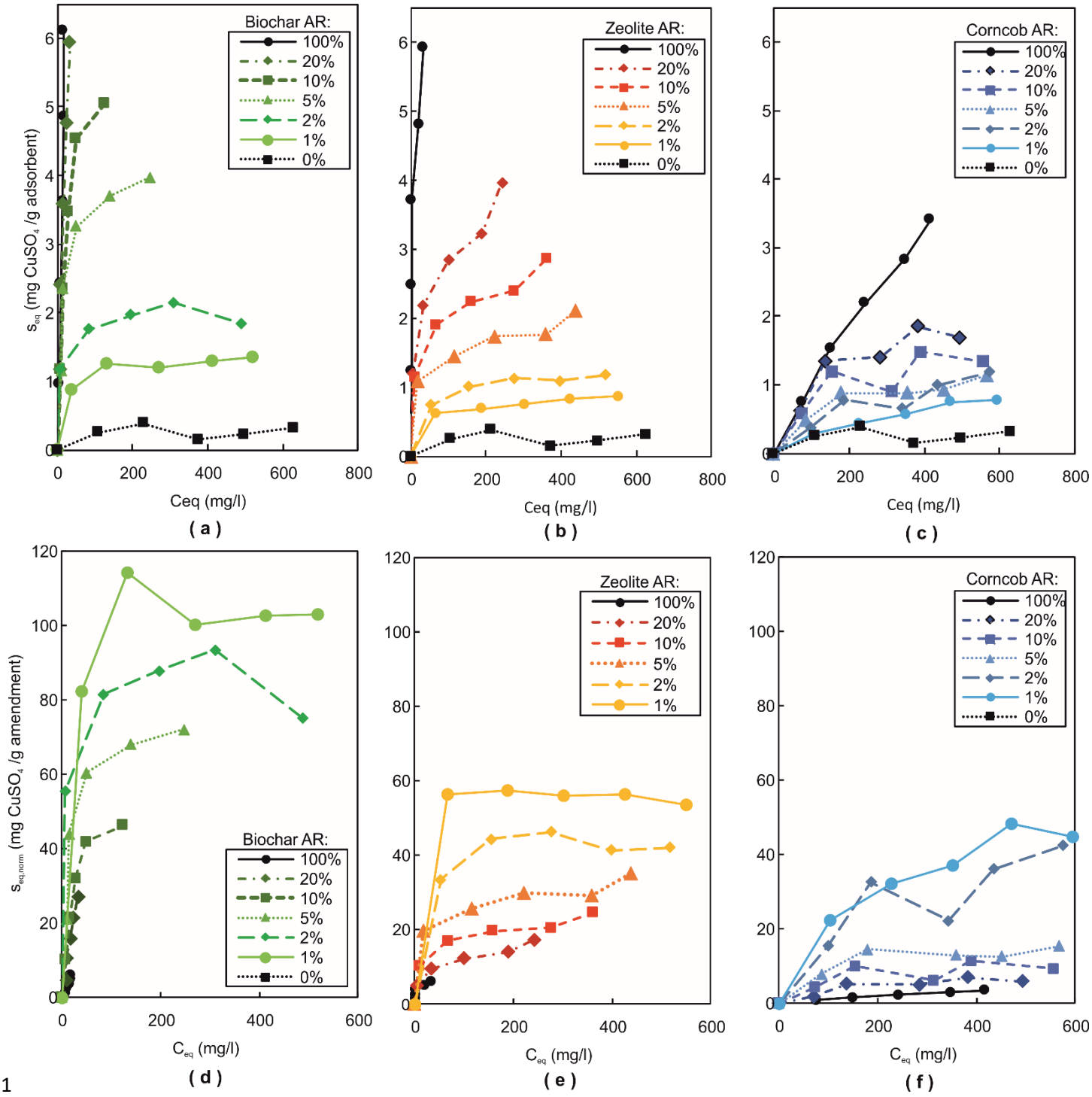
666



667

668 *Figure 2 Bulk density (a), water holding capacity (b), electrical conductivity (c) and pH (d) for amendment-*
669 *sand mixtures at different application rates*

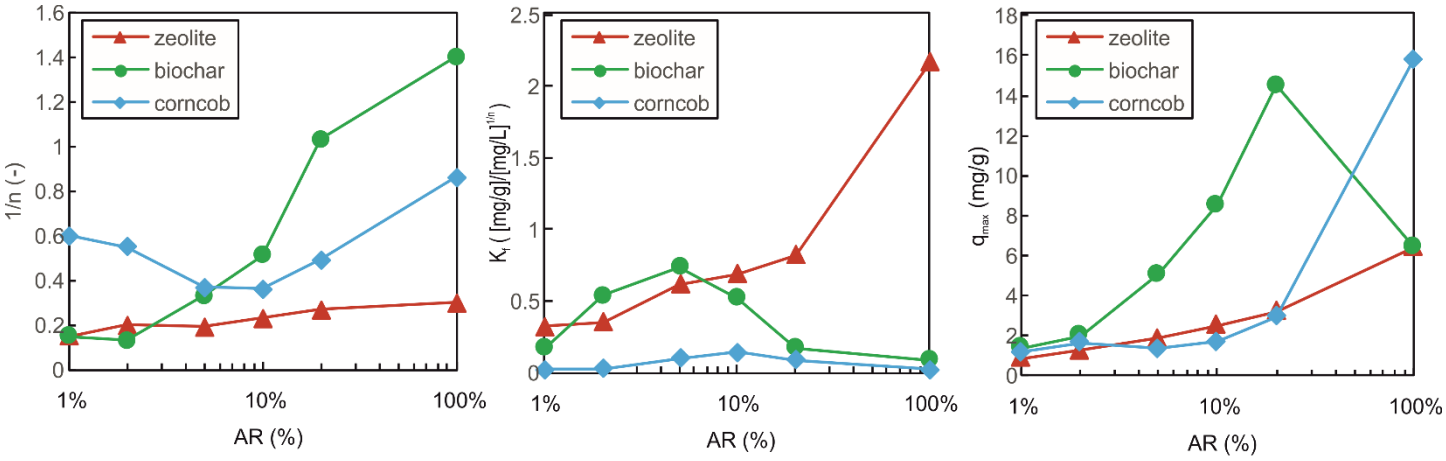
670



671

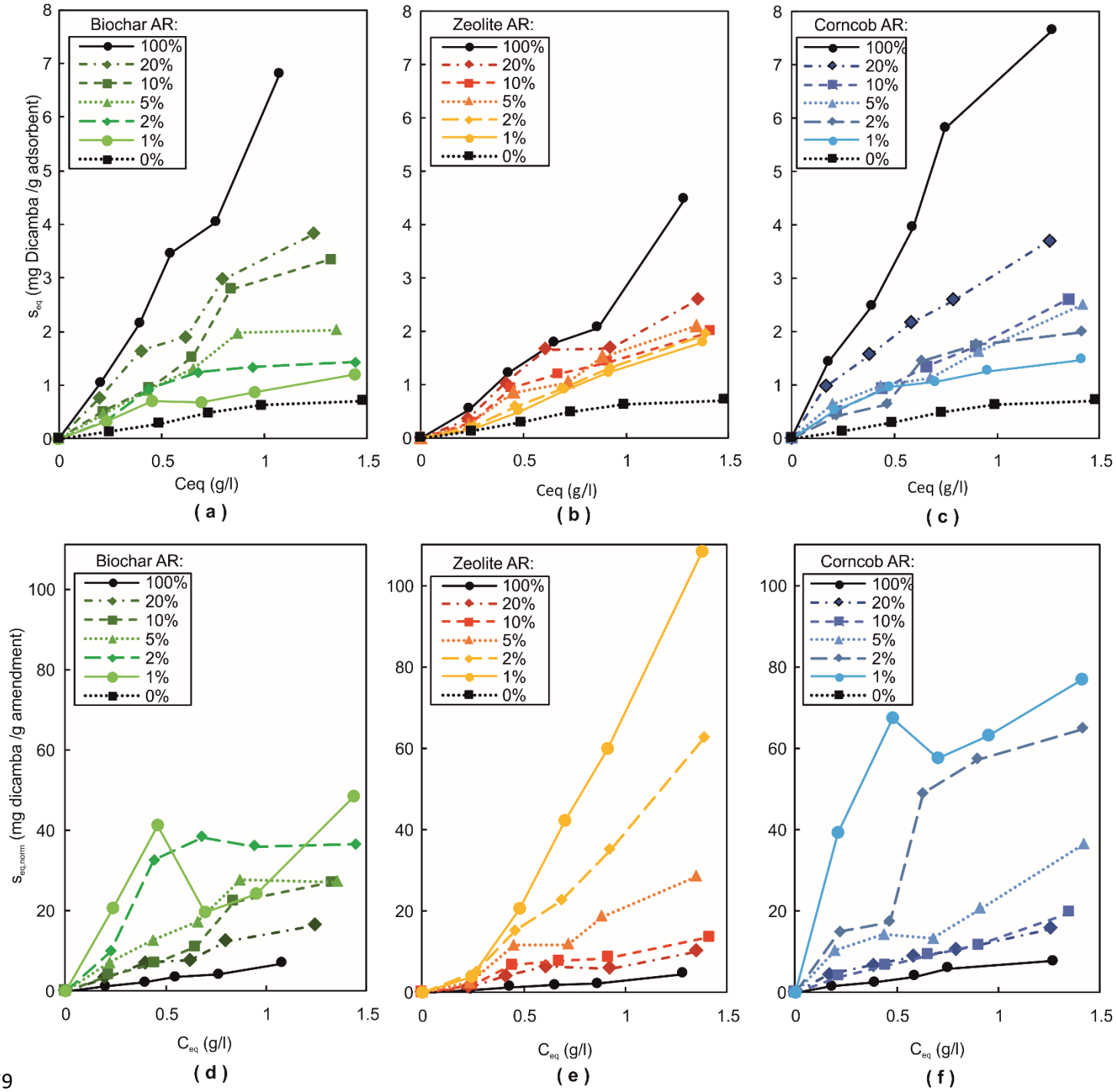
672 *Figure 3 Copper sulphate adsorption isotherms reported as adsorbed $CuSO_4$ per total mass of adsorbent (sand*
673 *+ amendment) (a-c) and per total mass of amendment (d-f) vs equilibrium concentration in liquid phase, at*
674 *different application rates (AR), for biochar (a,d), zeolite (b,e) and corncob (c,f)*

675



676

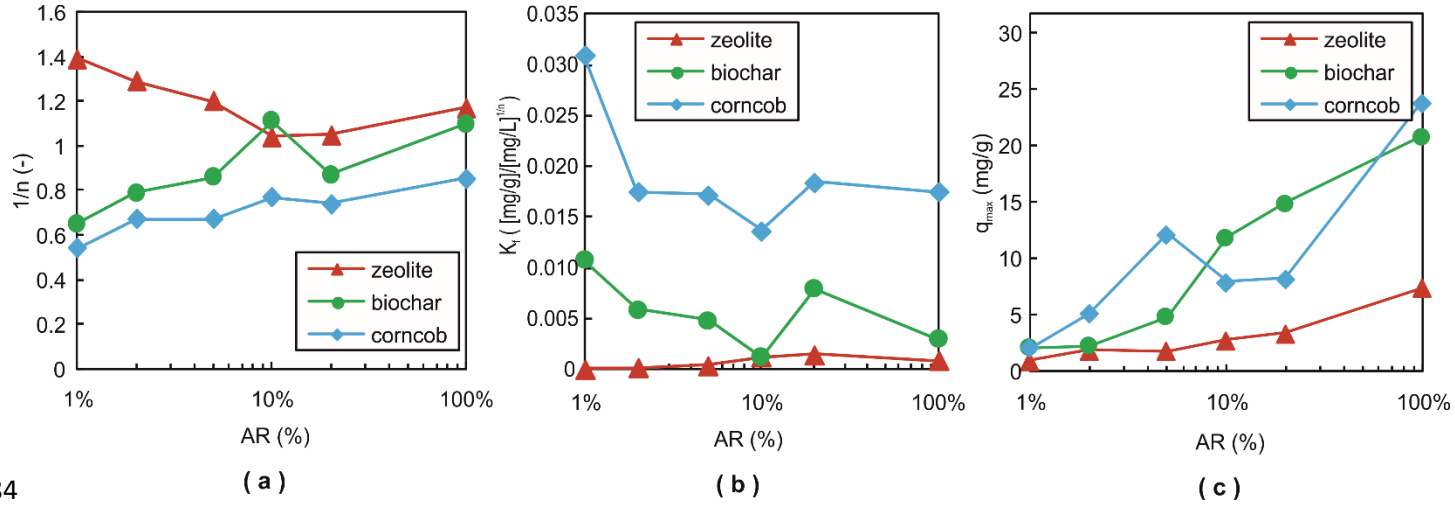
677 *Figure 4 Freundlich (a,b) and Langmuir (c) parameters for $CuSO_4$ adsorption isotherms as a function of the*
678 *amendment application rate*



679

680 *Figure 5 Dicamba adsorption isotherms reported as adsorbed dicamba per total mass of adsorbent (sand +*
681 *amendment) (a-c) and per total mass of amendment (d-f) vs equilibrium concentration in liquid phase, at*
682 *different application rates (AR), for biochar (a,d), zeolite (b,e) and corncob (c,f)*

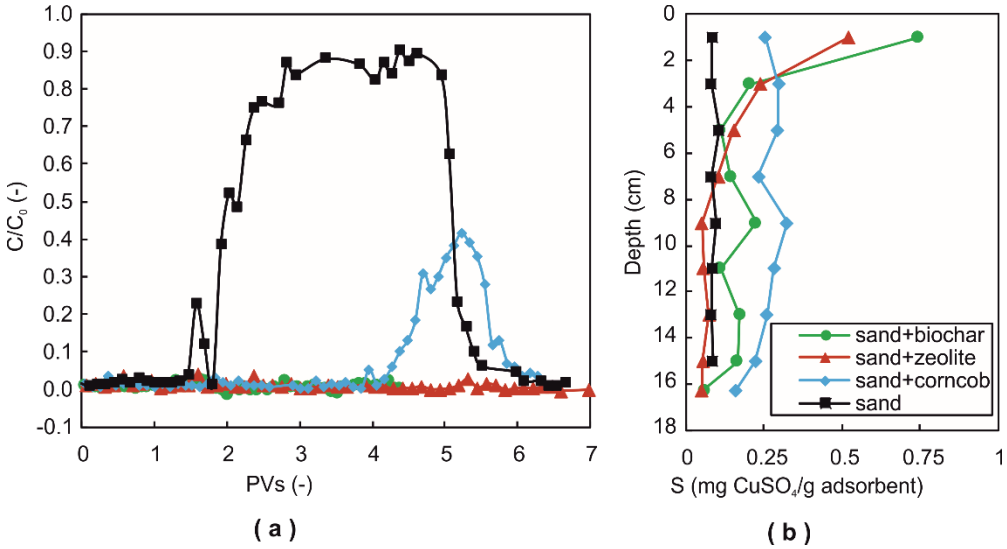
683



684

685 *Figure 6 Freundlich (a,b) and Langmuir (c) parameters for dicamba adsorption isotherms as a function of the*
686 *amendment application rate*

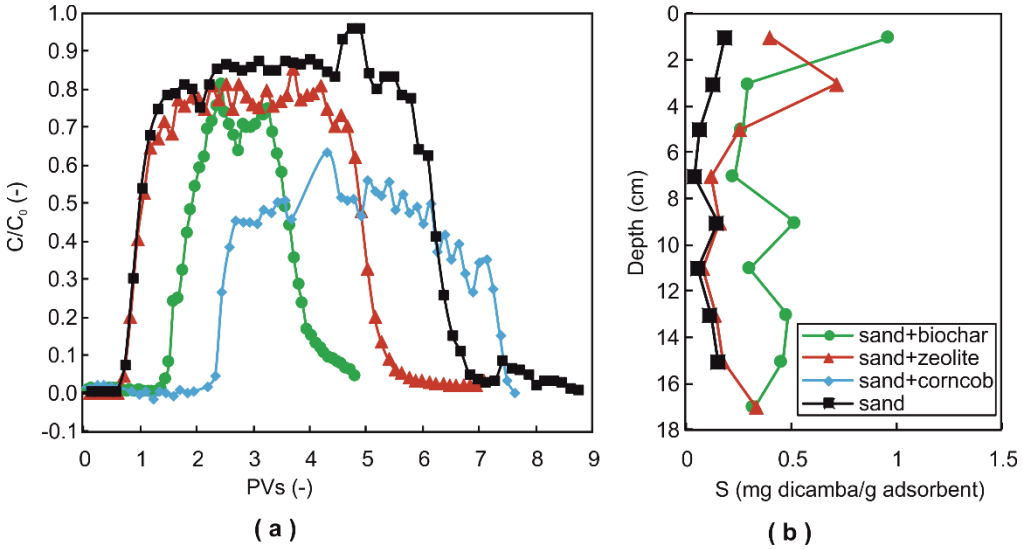
687



688

689 *Figure 7 Normalized $CuSO_4$ breakthrough curve (C/C_0 as a function of the number of injected pore volumes*
690 *PVs) (a) and final vertical profile of adsorbed $CuSO_4$ (mass concentration S versus depth) (b) for sand and sand-*
691 *amendment column leaching tests. The injection starts at PV = 0 (column pre-conditioning and tracer tests*
692 *are not reported)*

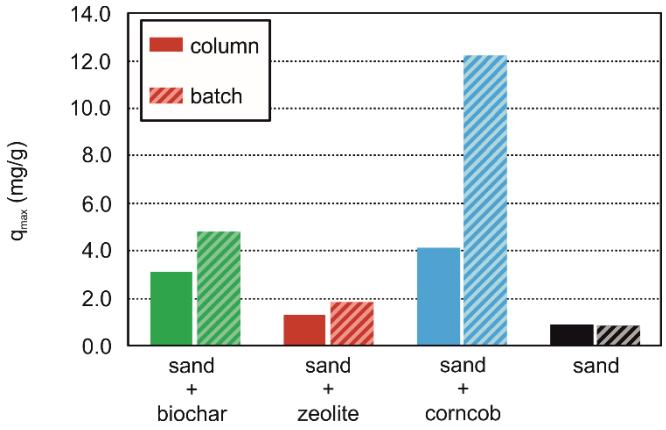
693



694

695 *Figure 8 Normalized dicamba breakthrough curve (C/C_0 as a function of the number of injected pore volumes*
696 *PVs) (a) and final vertical profile of adsorbed dicamba(mass concentration S versus depth) (b) for sand and*
697 *sand-amendment column leaching tests. The injection starts at PV = 0 (column pre-conditioning and tracer*
698 *tests are not reported)*

699



700

701 *Figure 9 Comparison of maximum adsorption capacity q_{max} obtained via fitting of breakthrough curves of*
702 *column transport tests (solid bars) and of adsorption isotherms of batch tests (dashed bars) of dicamba*
703 *solutions in contact with sand-amendment mixtures (application rate equal to 5%) and pure sand.*

704

705 # TABLE CAPTION

706 *Table 1 Column leaching tests: geometical characteristics, hydrodynamic parameters and mass balance*
707 *results*

708

	Sand	Zeolite-sand	Biochar-sand	Corncob-sand
$CuSO_4$				
Column length (cm)	15	16.5	18	18
Bulk density (g/cm^3)	1.54	1.40	1.28	1.28
Porosity (-)	0.41	0.42	0.485	0.44
Pore volume PV (min)	132	117	193	142
Unsaturated water content (-)	0.22	0.216	0.32	0.23
Saturated hydraulic conductivity K_{sat} (m/s)	$7.92 \cdot 10^{-5}$	$5.72 \cdot 10^{-5}$	$2.59 \cdot 10^{-5}$	$5.88 \cdot 10^{-5}$
Hydrodynamic dispersivity α (m)	$4.16 \cdot 10^{-3}$	$5.38 \cdot 10^{-3}$	$5.99 \cdot 10^{-3}$	$2.85 \cdot 10^{-3}$
Leached $CuSO_4$ (%)	56	1.2	1.1	10.2
Recovered $CuSO_4$ (leached + extracted) (%)	101.4	37.7	53.4	75.6
Dicamba				
Column length (cm)	15.4	17	18.2	18.5
Bulk density (g/cm^3)	1.50	1.36	1.27	1.25
Porosity (-)	0.40	0.41	0.48	0.44
Pore volume PV (min)	101	125	197	122
Unsaturated water content (m^3/m^3)	0.19	0.21	0.31	0.2
Saturated hydraulic conductivity K_{sat} (m/s)	$1.01 \cdot 10^{-4}$	$6.32 \cdot 10^{-5}$	$2.70 \cdot 10^{-5}$	$9 \cdot 10^{-5}$
Hydrodynamic dispersivity α (m)	$4.67 \cdot 10^{-3}$	$4.34 \cdot 10^{-3}$	$4.32 \cdot 10^{-3}$	$7.58 \cdot 10^{-3}$
Leached dicamba (%)	87	70	45.4	44
Recovered dicamba (leached + extracted) (%)	99	98.1	45.4*	88.9

709 * Dicamba vertical profile was not determined